ELECTRONIC SUPPORTING INFORMATION

Molybdenum Chloride Double Perovskites: Dimensionality Control of Optical and Magnetic Properties

Devesh Chandra Binwal,[a] Prashurya Pritam Mudoi,[a] Debendra Prasad Panda,[b] and Pratap Vishnoi*[a]

[a]New Chemistry Unit, International Centre for Materials Science & and School of Advanced Materials, Jawaharlal Nehru Centre for Advanced Scientific Research, Jakkur P.O. Bangalore-560064, India
Email: pvishnoi@jncasr.ac.in

[b] School of Advanced Materials & Chemistry and Physics of Materials Unit, Jawaharlal Nehru Centre for Advanced Scientific Research (JNCASR), Jakkur P. O., Bangalore 560064, India

Experimental section

Materials

Synthesis of $Cs_2NaMoCl_6$

Synthesis of $(MA)_2AgMoCl_6$

Synthesis of $(1,4\text{-}BDA)_2AgMoCl_8$

Synthesis of $(MA)_4MoCl_6{\cdot}Cl$

Single crystal X-ray diffraction

Powder X-ray diffraction

X-ray photoelectron spectroscopy (XPS)

Absorption spectroscopy

Raman spectroscopy

Thermogravimetric analysis (TGA)

Differential scanning calorimetery (DSC)

Magnetic measurements

Table S1: Single crystal data and structure refinement details of $Cs_2NaMoCl_6$

Table S2: Single crystal data and structure refinement details of $(MA)_2AgMoCl_6$

Table S3: Single crystal data and structure refinement details of $(1,4\text{-}BDA)_2AgMoCl_8$

Table S4: Single crystal data and structure refinement details of $(1,4\text{-}BDA)_2AgMoCl_8$ at 460 K

Table S5: Single crystal data and structure refinement details of $(MA)_4MoCl_6{\cdot}Cl$

Table S6: Bond distances and bond angles obtained from single crystal X-ray data

Table S7: Shortest N···Cl distance (in Å) in $(1,4\text{-}BDA)_2AgMoCl_8$.

Table S8: XPS data (in eV)

Table S9: Raman shifts (in cm^{-1})

Table S10: Comparison of unit cell lengths (Å) and angles (°) obtained from scXRD and Le Bail fitting of the experimental PXRD patterns

Figure S1: Simulated and experimental PXRD patterns of $Cs_2NaMoCl_6$

Figure S2: Simulated and experimental PXRD patterns of $(MA)_2AgMoCl_6$

Figure S3: Simulated and experimental PXRD patterns of $(1,4\text{-}BDA)_2AgMoCl_8$

Figure S4: TGA curve of $Cs_2NaMoCl_6$

Figure S5: Ambient stability studies of $Cs_2NaMoCl_6$ (a) optical images (b) X-ray photoelectron spectra of Mo 3d states and (c) Powder X-ray diffraction patterns; before and after exposure to ambient air for 4 weeks

Experimental section

***Materials*.** Molybdenum (III) chloride (Alfa Aesar, 99.5%), silver acetate (Sigma Aldrich, 99%), 1,4-butanediamine (Sigma Aldrich, 99%), sodium chloride (Sigma Aldrich, ≥ 99%), caesium chloride (Sigma Aldrich, 99.9%), methylamine hydrochloride (Sigma Aldrich, ≥ 98%), 50 wt.% H_3PO_2 in H_2O (Sigma Aldrich) and 37 wt.% HCl in H_2O (Merck, India) were purchased from commercial sources. All the compounds reported here were synthesized hydrothermally as single crystals and structurally characterized from single crystal x-ray diffraction data.

Synthesis of $Cs_2NaMoCl_6$. CsCl (168.30 mg, 1 mmol), $MoCl_3$ (101.30, 0.5 mmol), NaCl (29.20 mg, 0.5 mmol) were mixed gently with 2 mL of 37 wt.% aqueous HCl and 100 μL (slight excess) of 50 wt.% aqueous H_3PO_2 in a 23 mL Teflon vial. Teflon vial was kept in a stainless-steel autoclave and heated in an oven at 160°C at a rate of 5°C/min for 48 h. The reaction was cooled to room temperature at a cooling rate 0.1°C/min and red colour crystals were obtained. The red crystals of $Cs_2NaMoCl_6$ were filtered out of the mother liquor and washed several times with ethanol and dried in a vacuum oven at 60°C.

Synthesis of $(MA)_2AgMoCl_6$. Methylamine hydrochloride (135 mg, 2 mmol), $MoCl_3$ (202.6, 1 mmol), Ag(OAc) (166.9 mg, 1 mmol) were gently mixed with 2 mL of 37 wt.% aqueous HCl and 50 wt.% aqueous H_3PO_2 (120 mg, 200 μL, 1.8 mmol, in slight excess) in a 23 mL Teflon vial which was then tightly closed in a stainless-steel autoclave. The reaction temperature was increased from room temperature to 160°C at a heating rate of 5°C/minute and heated at this temperature for 48 h. After 48 h of continuous heating, the autoclave was cooled to room temperature at a cooling rate 0.1°C/min to obtain $(MA)_2AgMoCl_6$ as red colour crystals. The crystals were filtered out of the mother liquor and washed several times with ethanol, dried in a vacuum oven at 60 °C and stored in glove box.

Synthesis of $(1,4\text{-}BDA)_2AgMoCl_8$. 1,4-Butanediamine (87.70 mg, 100 μL, 1 mmol), $MoCl_3$ (101.30 mg, 0.5 mmol), Ag(OAc) (83.45 mg, 0.5 mmol) was mixed gently with 2 mL of 37 wt.% aqueous HCl and 100 μL (slight excess) of 50 wt.% aqueous H_3PO_2 in a 23 mL Teflon vial. Teflon vial was kept in a stainless-steel autoclave and heated in an oven at 160°C at a rate of 5.0°C/min for 48 h. The reaction was cooled to room temperature at a cooling rate 5.0°C/min and red colour crystals of $(1,4\text{-}BDA)_2AgMoCl_8$ were obtained. The red crystals were filtered out of the mother liquor and washed several times with ethanol and dried in a vacuum oven at 60°C.

Synthesis of $(MA)_4MoCl_6 \cdot Cl$. Methylamine hydrochloride (270 mg, 4.0 mmol), $MoCl_3$ (202.3 mg, 1.0 mmol), 37 wt.% aqueous HCl (2.0 mL) and 50 wt.% aqueous H_3PO_2 (120 mg, 200 μL, 1.8 mmol, in slight excess) were taken in a 23 mL Teflon vial. The vial was closed in a stainless-steel autoclave and placed in a temperature-programmable electric oven at 160 °C. The temperature of the oven was increased upto 160 °C at a heating rate of 5°C/minute and held at this temperature for 48 h. Red crystals of $(MA)_4MoCl_6 \cdot Cl$ were obtained after slow cooling the oven to room temperature at a cooling rate 0.1°C/minute. The crystals were filtered out of the mother liquor, washed several times with absolute ethanol, dried in a vacuum oven at 60 °C, and stored in a nitrogen filled glove box.

Single crystal X-ray diffraction. Single crystals of each sample were mounted on a quartz fibre with the help of silicon grease on a Bruker D8 Venture diffractometer equipped with photon detector and graphite-monochromatic Mo-Kα x-ray source (λ = 0.71073 Å). The data were collected at room temperature for all the compounds and at 460 K for sample $(1,4\text{-BDA})_2AgMoCl_8$ and integrated by using *APEX-3* software. *XPREP* was used to check for possibility of higher symmetry. The data were solved and refined by using *SHELX* 14.0.[1] All non-hydrogen atoms were refined anisotropically. The crystal structure figures were drawn by using *VESTA* 3.5.7.[2]

Powder X-ray diffraction. Crystals were powered in mortar and pestle before placing in PXRD sample holder. The PXRD data were collected on a Rigaku instrument (Smart Lab) equipped with a Cu-Kα x-ray source (λ = 1.54059 Å). The experimental powder diffraction data were fitted to the simulated powder pattern from the single crystal x-ray diffraction data by using GSAS-II software. The data were plotted in qtgrace.

X-ray photoelectron spectroscopy (XPS). The XPS data of the sample $(1,4\text{-BDA})_2AgMoCl_8$ was collected on a Thermo scientific K-Alpha x-ray photoelectron spectrometer equipped with a monochromated, micro-focused, low-power Mg-Kα x-ray source. The spectra of $Cs_2NaMoCl_6$, $(MA)_2AgMoCl_6$ and $(MA)_4MoCl_6 \cdot Cl$ were collected on Omicron NanoTechnology spectrometer by using Mg-Kα x-ray source. The samples were powdered and then mounted on the XPS sample holder by using double-sided copper tape. Survey scan spectra were measured in the 10 eV-1000 eV range and for each sample core level spectra were recorded. The data were fitted by using fityk software and plotted in qtgrace software.

Raman spectroscopy. Raman spectra of all the samples were measured on HORIBA Lab-Ram HR800 spectrometer by using a laser of wavelength 514.5 nm as an excitation source. The Raman spectrum of silicon standard was also collected for reference purposes.

Absorption spectroscopy. Powder sample and $BaSO_4$ were taken in a ratio of 1:3 and mixed in mortar and pestle to dilute the sample. Diffuse reflectance UV spectroscopy experiments were performed on the mixture in the range of 200 nm to 1000 nm where $BaSO_4$ was used as a reference for 100% reflectance. Band gap for theses samples were calculated by conversion of reflectance to absorption by Kubelka–Munk equation: $\alpha/S = (1 - R)^2(2R)^{-1}$.

Thermogravimetric analysis (TGA). The TGA data of $(1,4\text{-BDA})_2AgMoCl_8$ were collected under an inert nitrogen atmosphere on a Mettler Toledo TGA 1 STAR^e instrument. 6.432 mg of the sample was taken in an alumina crucible and heated from room temperature to 900 °C at a heating rate of 10 °C/minute.

Differential scanning calorimetery (DSC) of $(1,4\text{-BDA})_2AgMoCl_8$. The DSC data of a powered sample of $(1,4\text{-BDA})_2AgMoCl_8$ were collected on a Mettler Toledo DSC 3 STAR^e system in the temperature range of -150 °C to 220 °C at a heating rate of 10 °C/minute under a continuous flow of liquid nitrogen at 40 ml/minute flow rate. 5.5 mg of the sample was taken for the measurement and sample was cooled first to -150 °C and then heated till 220 °C. Three cycles of data were collected to ascertain repeatability.

Magnetic measurements. Magnetic measurements were performed for powered samples in the temperature range of 2 K to 300 K on a SQUID magnetic property measurement system (MPMS 3) with VSM mode (Quantum Design, USA). Zero-field cooled (ZFC) and field cooled (FC) measurements were carried out with an applied field of 1000 Oe. Magnetic susceptibility χ *vs.* T has been transformed to the effective magnetic moment using the equation-

$$m_{eff} = \sqrt{\frac{3k_B}{N_A\mu_B^2}\chi T}$$

where k_B is the Boltzmann constant, χ is the molar susceptibilities, T is the temperature, N_A is Avogadro's number and μ_B is Bohr magneton.

Table S1: Single crystal data and structure refinement details of $Cs_2NaMoCl_6$.

Empirical formula	$Cs_4Na_2Mo_2Cl_{12}$
Formula weight	1194.90
Temperature	300(2) K
Crystal system	Cubic
Space group	$Fm\bar{3}m$
Unit cell dimensions	10.41290(10) Å
Volume	1129.05(3) $Å^3$
Z	2
Density (calculated)	3.515 mg/m^3
Absorption coeff.	8.908 mm^{-1}
θ range	3.389 to 33.096°
Reflections collected	210
Independent reflections	143 [R(int) = 0.0057]
Data completeness	98.7 %
Data/restraints /parameters	143 / 0 / 8
GoF on F^2	1.225
Final R indices [I>2sigma(I)]	$R1$ = 0.0136 $wR2$ = 0.0371
R indices (all data)	$R1$ = 0.0161 $wR2$ = 0.0382

Table S2: Single crystal data and structure refinement details of $(MA)_2AgMoCl_6$.

Empirical formula	$C_2H_{12}N_2AgMoCl_6$
Formula weight	480.65
Temperature	293(2) K
Crystal system	Trigonal
Space group	$P\bar{3}m1$
Unit cell dimensions	
a	7.3359(2) Å
b	7.3359(2) Å
c	6.8017(2) Å
α	90°
β	90°
γ	120°
Volume	317.00(2) $Å^3$
Z	1
Density (calculated)	2.518 mg/m^3
Absorption coeff.	3.753 mm^{-1}
θ range	2.995 to 27.019°
Reflections collected	6077
Data / restraints /parameters	287 / 0 / 19
Independent reflections	287 [R(int) = 0.0241]
Data completeness	97.6 %
GoF on F^2	1.373
Final R indices [I>2sigma(I)]	R1 = 0.0368 wR2 = 0.0964
R indices (all data)	R1 = 0.0369 wR2 = 0.0964

Table S3: Single crystal data and structure refinement details of $(1,4\text{-BDA})_2AgMoCl_8$.

Empirical formula	$C_8H_{28}N_4AgMoCl_8$
Formula weight	667.75
Temperature	293(2) K
Crystal system	Triclinic
Space group	$P\bar{1}$
Unit cell dimensions	
a	7.6668(15) Å
b	7.7072(14) Å
c	9.4490(14) Å
α	102.229(8)°
β	91.183(6)°
γ	90.127(6)°
Volume	545.54(17) $Å^3$
Z	1
Density (calculated)	2.033 mg/m^3
Absorption coeff.	2.451 mm^{-1}
θ range	2.657 to 30.605°
Reflections collected	28316
Data / restraints /parameters	3316 [R(int) = 0.0341]
Independent reflections	98.5 %
Data completeness	3316 / 0 / 103
GoF on F^2	1.187
Final R indices [I>2sigma(I)]	$R1$ = 0.0396, $wR2$ = 0.1180
R indices (all data)	$R1$ = 0.0410, $wR2$ = 0.1188

Table S4: Single crystal data and structure refinement details of $(1,4\text{-BDA})_2AgMoCl_8$ at 460 K.

Empirical formula	$C_8H_{28}N_4AgMoCl_8$
Formula weight	667.75
Temperature	460(2) K
Crystal system	Triclinic
Space group	$P\bar{1}$
Unit cell dimensions	
a	7.636(2) Å
b	7.671(2) Å
c	9.789(3) Å
α	80.191(12)°
β	88.082(12)°
γ	89.402(12)°
Volume	564.7(3) $Å^3$
Z	1
Density (calculated)	1.964 mg/m^3
Absorption coeff.	2.368 mm^{-1}
θ range	2.669 to 27.557°
Reflections collected	26795
Data / restraints /parameters	2584 / 1 / 78
Independent reflections	2584 [R(int) = 0.0899]
Data completeness	100.0 %
GoF on F^2	1.05
Final R indices [I>2sigma(I)]	R1 = 0.0419 wR2 = 0.1181
R indices (all data)	R1 = 0.0696 wR2 = 0.1294

Table S5: Single crystal data and structure refinement details of $(MA)_4MoCl_6 \cdot Cl$.

Empirical formula	$C_4H_{24}N_4MoCl_7$
Formula weight	472.36
Temperature	300(2) K
Crystal system	Monoclinic
Space group	*P*2/n
Unit cell dimensions	
a	16.0647(9) Å
b	7.3477(4) Å
c	16.1264(8) Å
α	90°
β	103.599(2)°
γ	90°
Volume	1850.17(17) $Å^3$
Z	4
Density (calculated)	1.696 mg/m^3
Absorption coeff.	1.705 mm^{-1}
θ range	2.046 to 27.132°
Reflections collected	83107
Data / restraints /parameters	4099 / 0 / 157
Independent reflections	4099 [R(int) = 0.0736]
Data completeness	100 %
GoF on F^2	1.037
Final R indices [I>2sigma(I)]	R1 = 0.0251 wR2 = 0.0496
R indices (all data)	R1 = 0.0410 wR2 = 0.0540

Table S6: Bond distances and bond angles obtained from single crystal x-ray data.

$Cs_2NaMoCl_6$	
Bond lengths (Å) Mo(1)-Cl(1) = 2.4474(9) Na(1)-Cl(1) = 2.7590(9) Nearest Mo···Mo = 7.36303(7)	*Bond angles* (°) Cl(1)-Mo(1)-Cl(1) = 90 & 180 Cl(1)-Na(1)-Cl(1) = 90 & 180
$(MA)_2AgMoCl_6$	
Bond lengths (Å) Mo(1)-Cl(1) = 2.447(2) Ag(1)-Cl(1) = 2.796(2) Nearest Mo···Mo = 6.8017(3)	*Bond angles* (°) Cl(1)-Mo(1)-Cl(1) = 90.75(7) & 89.25(7) Cl(1)-Ag(1)-Cl(1) = 104.12(6) & 75.88(6) Cl(1)-Mo(1)-Cl(1) = Cl(1)-Ag(1)-Cl(1) = 180
$(1,4\text{-BDA})_2AgMoCl_8$	
Bond lengths (Å) Mo(1)-Cl(1) = 2.4476(10) Mo(1)-Cl(3) = 2.4521(9) Mo(1)-Cl(4) = 2.4462(9) Ag(1)-Cl(2) = 2.4447(11) Ag(1)-Cl(3) = 3.0472(11) Ag(1)-Cl(4) = 3.0406(11) Nearest Mo···Mo = 7.6668(16)	*Bond angles* (°) Cl(1)-Mo(1)-Cl(3) = 90.94(4) & 89.06(4) Cl(1)-Mo(1)-Cl(4) = 90.58(4) & 89.42(4) Cl(3)-Mo(1)-Cl(4) = 90.41(4) & 89.59(4) Cl(2)-Ag(1)-Cl(3) = 91.73(4) & 88.27(4) Cl(2)-Ag(1)-Cl(4) = 93.49(4) & 86.51(4) Cl(3)-Ag(1)-Cl(4) = 91.60(3) & 88.40(3) Cl(1)-Mo(1)-Cl(1) = Cl(2)-Ag(1)-Cl(2) = Cl(3)-Mo(1)-Cl(3) = Cl(4)-Mo(1)-Cl(4) = 180
$(1,4\text{-BDA})_2AgMoCl_8$ at 460K	
Bond lengths (Å) Mo(1)-Cl(1) = 2.4475(17) Mo(1)-Cl(3) = 2.4476(13) Mo(1)-Cl(4) = 2.4439(14) Ag(1)-Cl(2) = 2.4786(18) Ag(1)-Cl(3) = 2.9965(16) Ag(1)-Cl(4) = 3.0081(16) Nearest Mo···Mo = 7.636(2)	*Bond angles* (°) Cl(1)-Mo(1)-Cl(2) = 90.28(6) & 89.72(6) Cl(1)-Mo(1)-Cl(3) = 90.64(5) & 89.36(5) Cl(2)-Mo(1)-Cl(3) = 90.44(5) & 89.56(5) Cl(2)-Ag(1)-Cl(4) = 88.50(6) & 91.50(6) Cl(2)-Ag(1)-Cl(3) = 88.76(6) & 91.24(6) Cl(3)-Ag(1)-Cl(4) = 90.90(5) & 89.10(5) Cl(1)-Mo(1)-Cl(1) = Cl(2)-Ag(1)-Cl(2) = 180 Cl(3)-Mo(1)-Cl(3) = Cl(4)-Mo(1)-Cl(4) = 180
$(MA)_4MoCl_6 \cdot Cl$	
Bond lengths (Å) Mo(1)-Cl(1) = 2.4515(6) Mo(1)-Cl(2) = 2.4459(6) Mo(1)-Cl(3) = 2.4519(6) Mo(2)-Cl(4) = 2.4490(6) Mo(2)-Cl(5) = 2.4466(8) Mo(2)-Cl(6) = 2.4488(6) Nearest Mo···Mo = 7.3477(5)	*Bond angles* (°) Cl(1)-Mo(1)-Cl(2) = 89.96(2) & 90.04(2) Cl(1)-Mo(1)-Cl(3) = 89.36(2) & 90.64(2) Cl(2)-Mo(1)-Cl(3) = 90.07(2) & 89.93(2) Cl(4)-Mo(2)-Cl(5) = 90.50(2) & 89.50(2) Cl(4)-Mo(2)-Cl(6) = 90.04(2) & 89.96(2) Cl(5)-Mo(2)-Cl(6) = 90.17(2) & 89.83(2) Cl(1)-Mo(1)-Cl(1) = Cl(2)-Mo(1)-Cl(2) = Cl(3)-Mo(1)-Cl(3) = Cl(4)-Mo(2)-Cl(4) = Cl(5)-Mo(5)-Cl(5) = Cl(6)-Mo(2)-Cl(6) = 180

Table S7: Shortest N···Cl distance (in Å) in $(1,4\text{-BDA})_2AgMoCl_8$. Shadow indicates N···Cl distance between N and the equatorial (bridging) Cl atoms.

Atoms	**Room temperature structure (300 K)**	**High temperature structure (460 K)**
N(1)-Cl(1)	3.747(5) & 3.986(5)	3.666(6) & 4.019(6)
N(1)-Cl(2)	3.176(5) & 4.530(5)	3.244(5) & 4.418(5)
N(1)-Cl(3)	3.508(5) & 3.686(4)	3.510(6) & 3.677(5)
N(1)-Cl(4)	3.333(4) & 3.381(5)	3.423(6) & 3.453(5)
N(2)-Cl(1)	3.238(5) & 4.485(5)	3.312(5) & 4.361(5)
N(2)-Cl(2)	4.364(6) & 3.378(6)	4.409(7) & 3.304(7)
N(2)-Cl(3)	3.381(5) & 3.401(6)	3.434(6) & 3.440(6)
N(2)-Cl(4)	3.354(5) & 3.902(5)	3.342(6) & 3.679(6)

Table S8: XPS data of the elements present (in eV).

XPS peaks	$Cs_2NaMoCl_6$	$(MA)_2AgMoCl_6$	$(1,4\text{-BDA})_2AgMoCl_8$	$(MA)_4MoCl_6.Cl$
Ag $3d_{5/2}$	-	367.4	367.5	-
Ag $3d_{3/2}$	-	373.4	373.5	-
Mo $3d_{5/2}$	229.5	229.2	229.5	229.4
Mo $3d_{3/2}$	232.7	232.4	232.7	232.7
Cl $2p_{3/2}$	197.6	197.5	197.8	197.5
Cl $2p_{1/2}$	199.2	199.1	199.5	199.1
Na 1*s*	1071.5	-	-	-
Cs $3d_{5/2}$	723.5	-	-	-
Cs $3d_{3/2}$	737.5	-	-	-
C 1*s*	284.6	284.6	284.6	284.6
N 1*s*	-	401.1	401.1	401.2

Table S9: Raman shifts (in cm^{-1}).

$Cs_2NaMoCl_6$	$(MA)_2AgMoCl_6$	$(1,4\text{-BDA})_2AgMoCl_8$	$(MA)_4MoCl_6{\cdot}Cl$
145.7	155.3	143.2	163
307.1	253.2	256.2	256.9
	294.4	294.2	292.4
	981.6	502.3	938.6
		795.8	997.8
		869.9	
		958.4	
		987.7	
		1066.3	

Table S10: Comparison of unit cell lengths (Å) and angles (°) obtained from scXRD and Le Bail fitting of the experimental PXRD patterns.

$Cs_2NaMoCl_6$		$(MA)_2AgMoCl_6$	
scXRD	***PXRD***	***scXRD***	***PXRD***
a = 10.41290(10)	*a* = 10.40918	*a* = 7.3359(2)	*a* = 7.33469
b = 10.41290(10)	*b* = 10.40918	*b* = 7.3359(2)	*b* = 7.33469
c = 10.41290(10)	*c* = 10.40918	*c* = 6.8017(2)	*c* = 6.80041
α = 90°	α = 90°	α = 90	α = 90
β = 90°	β = 90°	β = 90	β = 90
γ = 90°	γ = 90°	γ = 120	γ = 120
$(1,4\text{-BDA})_2AgMoCl_8$		$(MA)_4MoCl_6.Cl$	
scXRD	***PXRD***	***scXRD***	***PXRD***
a = 7.6668(15)	*a* = 7.66584	*a* = 16.0659(9)	*a* = 16.05688
b = 7.7072(14)	*b* = 7.7067	*b* = 7.3481(4)	*b* = 7.3515
c = 9.4490(14)	*c* = 9.45378	*c* = 16.1273(8)	*c* = 16.12647
α =102.229(8)	α = 102.364	α = 90°	α = 90°
β = 91.183(6)	β = 91.244	β = 103.601(2)°	β = 103.587
γ = 90.127(6)	γ = 90.148	γ = 90°	γ = 90°

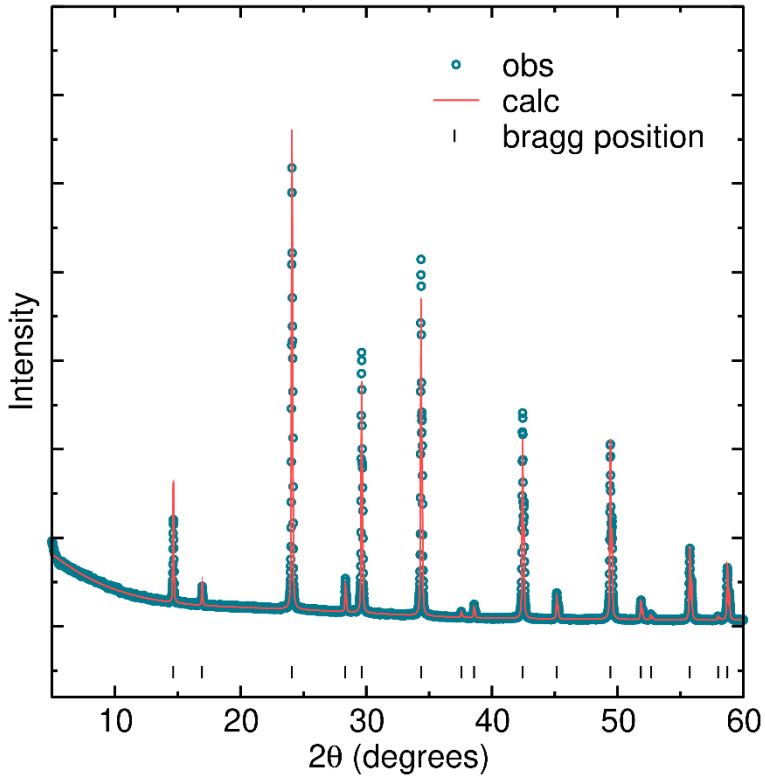

Figure S1: Simulated and experimental PXRD patterns of $Cs_2NaMoCl_6$.

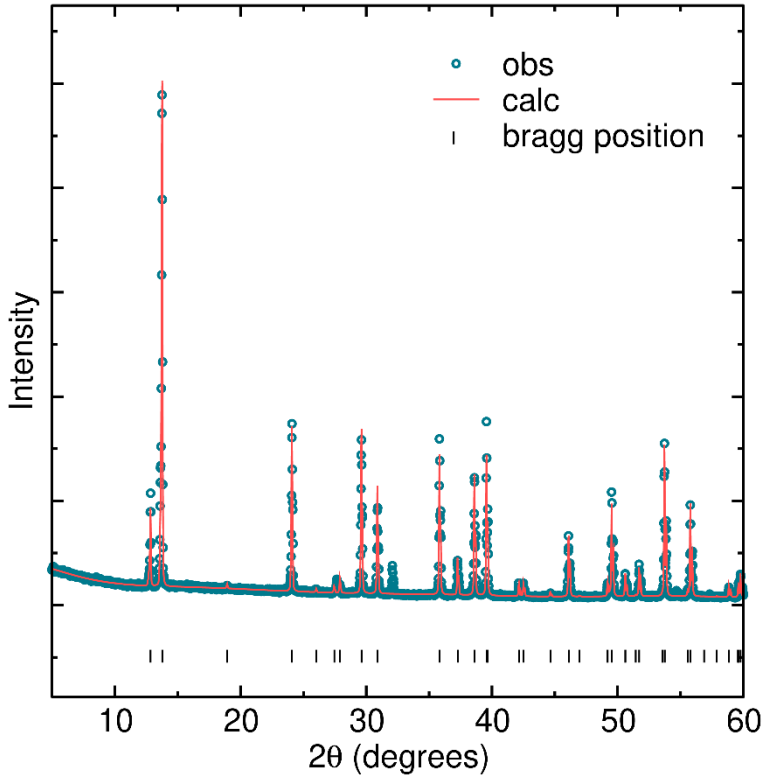

Figure S2: Simulated and experimental PXRD patterns of $(MA)_2AgMoCl_6$.

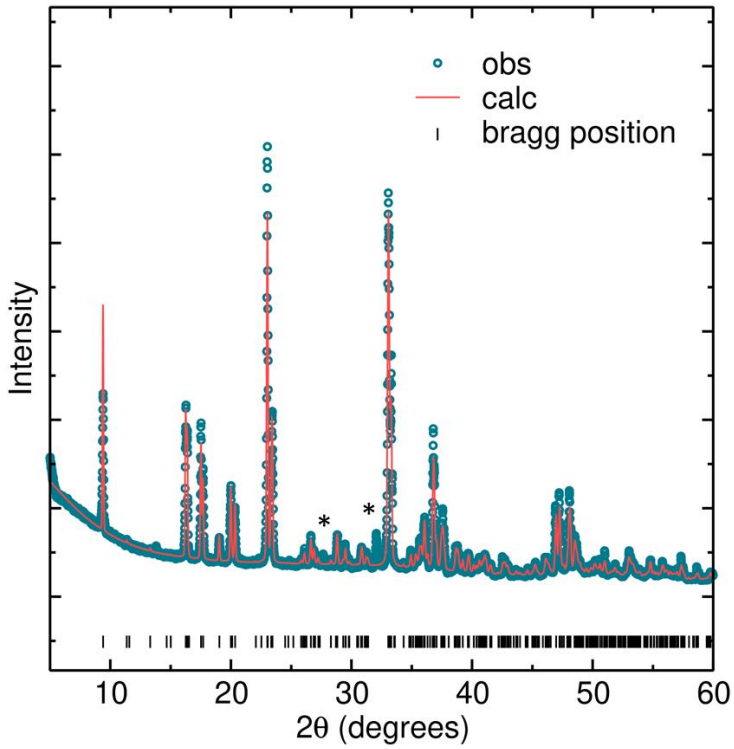

Figure S3: Simulated and experimental PXRD patterns of (1,4-BDA)$_2$AgMoCl$_8$. Small impurity of AgCl has also been observed which is marked by black asterisk.

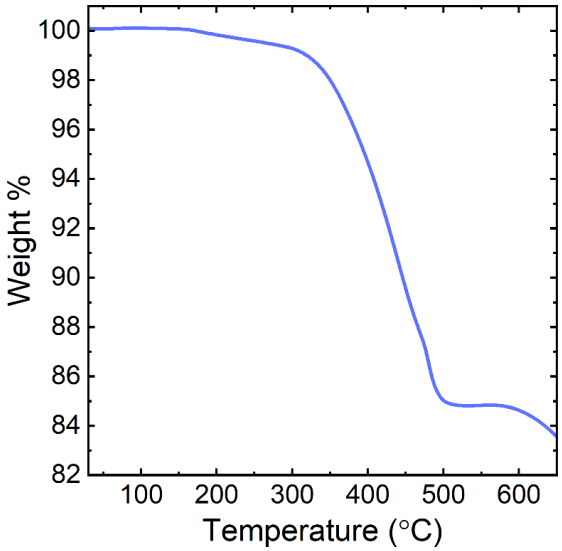

Figure S4: TGA curve of Cs$_2$NaMoCl$_6$.

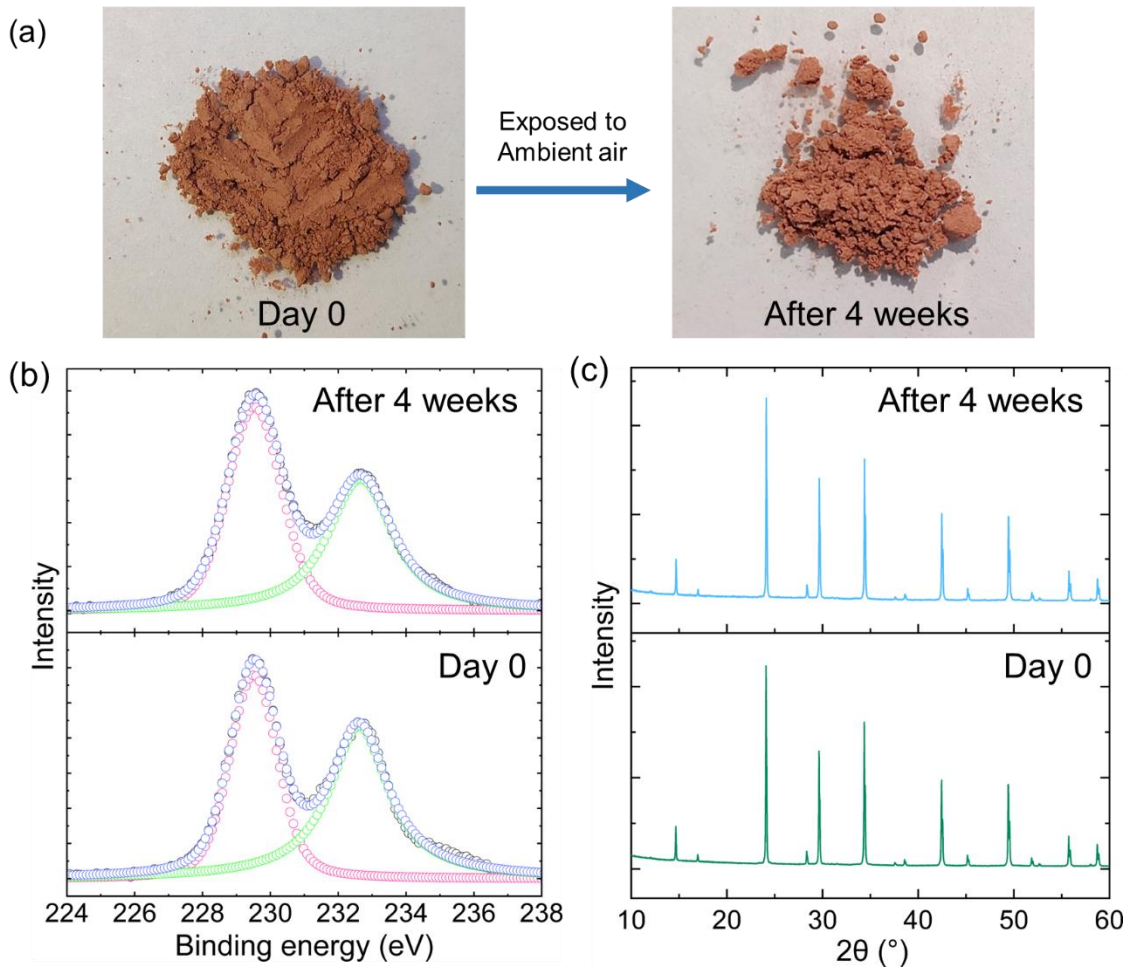

Figure S5: Ambient stability studies of $Cs_2NaMoCl_6$ (a) optical images (b) X-ray photoelectron spectra of Mo 3d states and (c) Powder X-ray diffraction patterns; before and after exposure to ambient air for 4 weeks.

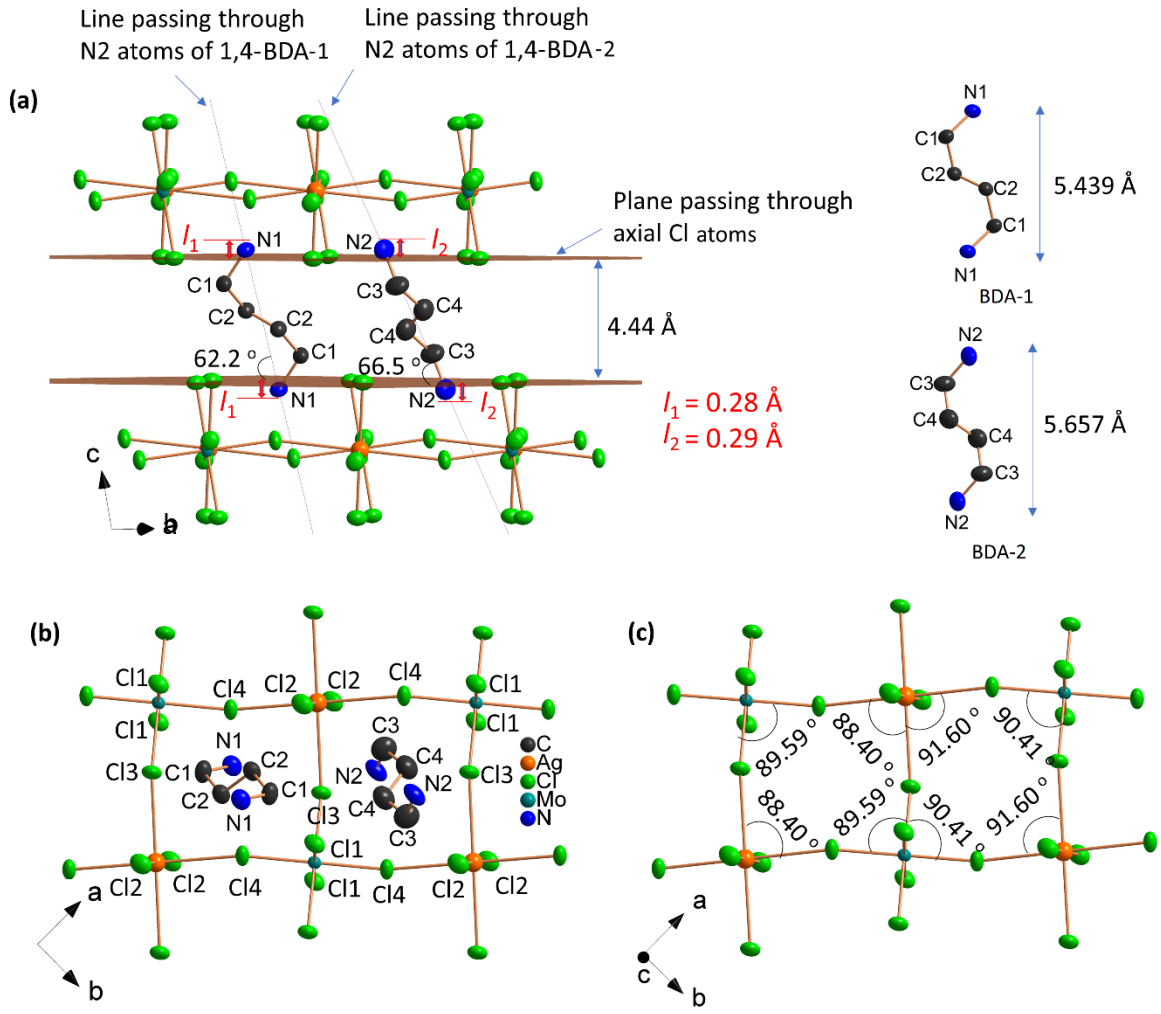

Figure S6: (a) Crystal structure of $(1,4\text{-BDA})_2AgMoCl_8$ at room temperature, showing penetration of 1,4-BDA cation in the perovskite layer. Probability (percentage) used for ellipsoid mode is 50%. H atoms are not shown for clarity. The structure exhibits crystallographically unique two 1,4-BDA cations, i.e. BDA-1 and BDA-2 which adopt *gauche* conformation. BDA-2 is longer with the distance between N-terminals is 5.657 Å, has larger thermal ellipsoids and higher depth of penetration (0.29 Å) into the plane passing through the axial Cl atoms of the perovskite layer. (b) and (c) shows that the cavity for BDA-2 is relatively larger than that for the cation BDA-1 because of the equatorial Cl-Ag-Cl and Cl-Mo-Cl bond angles are larger.

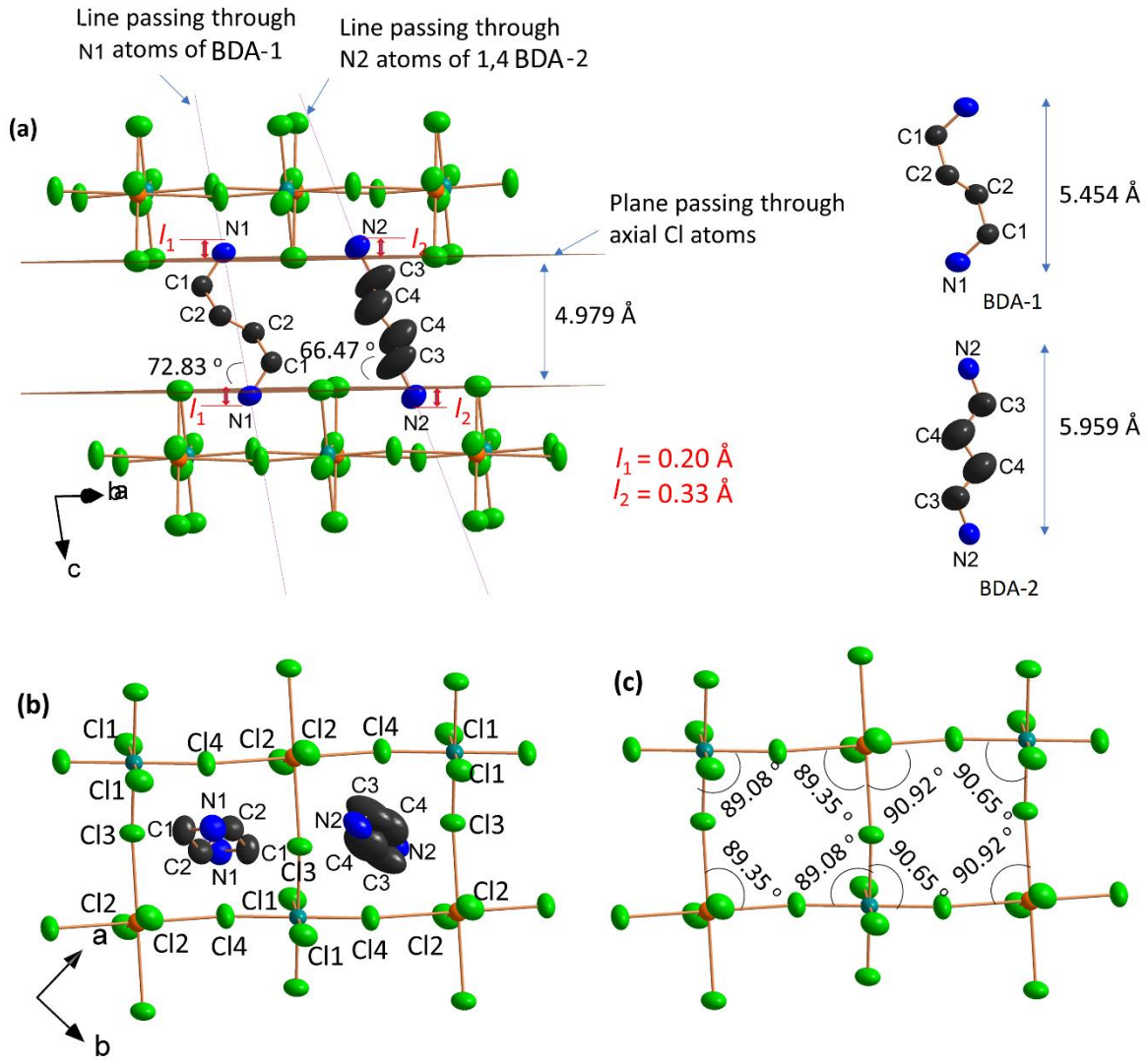

Figure S7: (a) Crystal structure of $(1,4\text{-BDA})_2AgMoCl_8$ at 460 K, showing penetration of 1,4-BDA cation in the perovskite layer. Probability (percentage) used for ellipsoid mode is 50%. H atoms are not shown for clarity. The structure exhibits crystallographically unique two 1,4-BDA cations, i.e. BDA-1 and BDA-2, adopting *gauche* and *anti* conformations, respectively. BDA-2 is longer with the distance between N-terminals is 5.959 Å, has larger thermal ellipsoids and higher depth of penetration (0.33 Å) into the plane passing through the axial Cl atoms of the perovskite layer. (b) and (c) shows that the cavity for BDA-2 is relatively larger than that for the cation BDA-1 because of the equatorial Cl-Ag-Cl and Cl-Mo-Cl bond angles are slightly larger. But the difference in the angles between two cavities is smaller in this structure than that of the room temperature structure which suggest that the perovskite layer is more symmetric at high temperature.

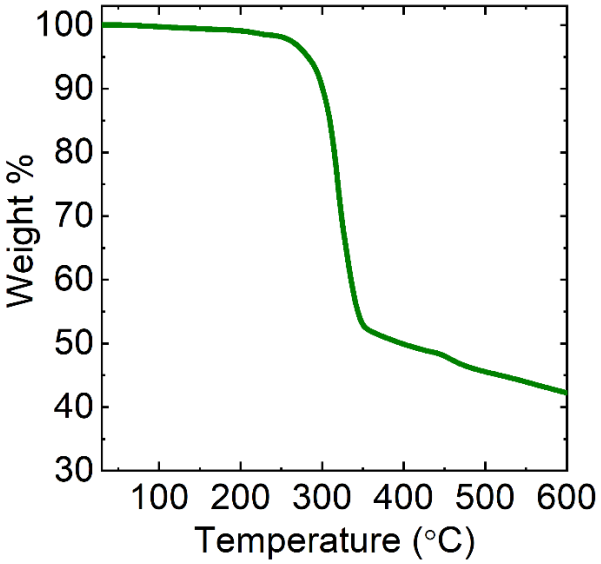

Figure S8: TGA curve of (1,4-BDA)$_2$AgMoCl$_8$.

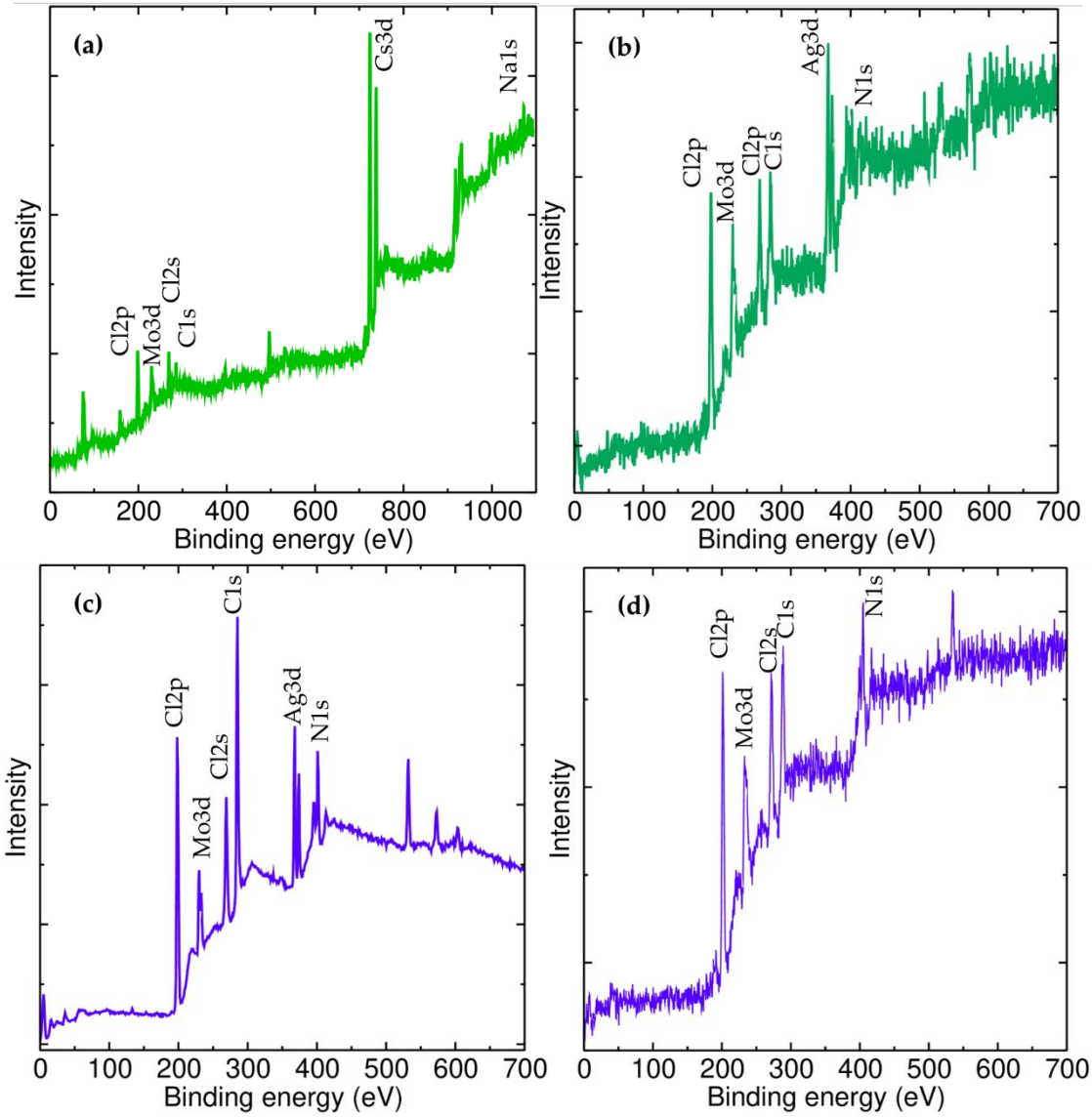

Figure S9: XPS survey spectra of (a) $Cs_2NaMoCl_6$, (b) $(MA)_2AgMoCl_6$, (c) (1,4-BDA)$_2AgMoCl_8$ and (d) $(MA)_4MoCl_6{\cdot}Cl$.

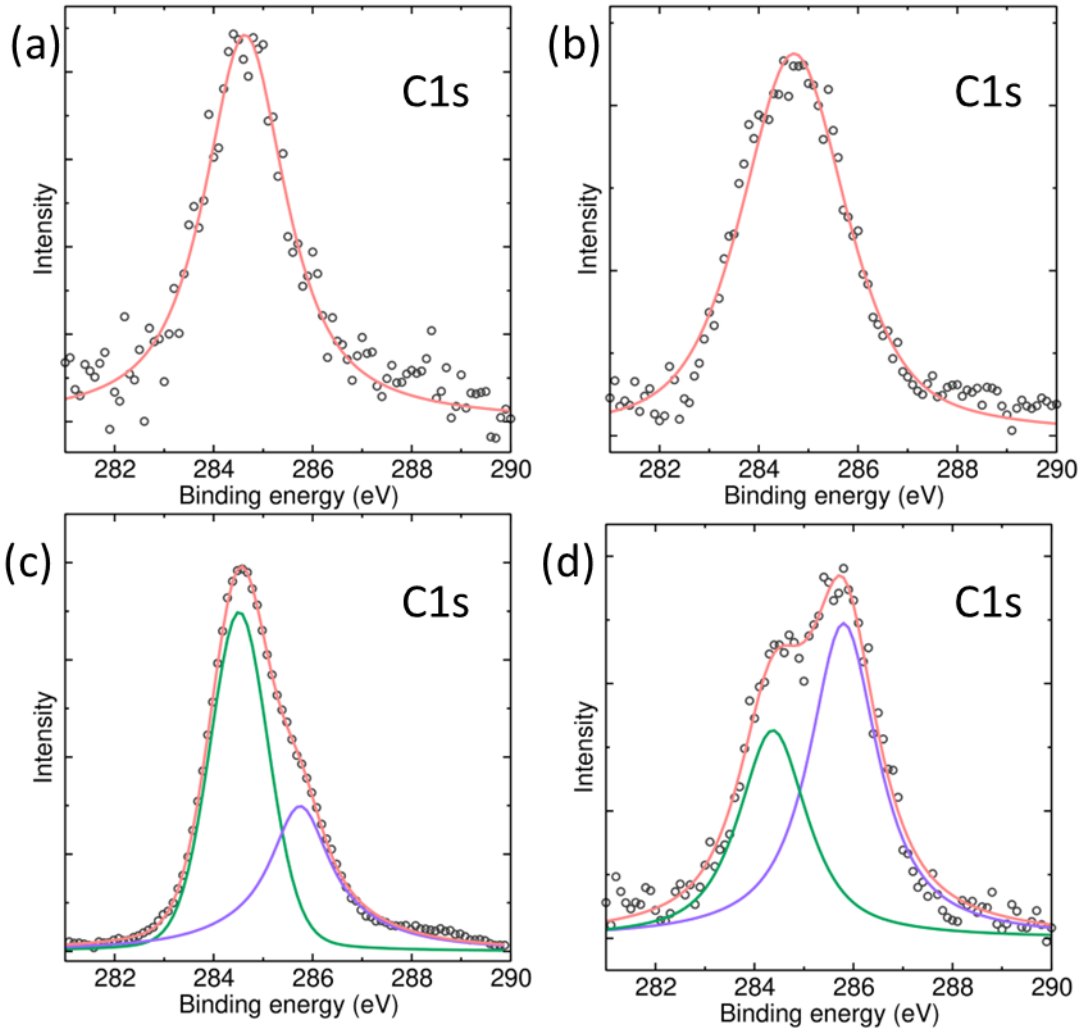

Figure S10: Core level C1s XPS spectra of (a) $Cs_2NaMoCl_6$, (b) $(MA)_2AgMoCl_6$, (c) $(1,4\text{-}BDA)_2AgMoCl_8$ and (d) $(MA)_4MoCl_6{\cdot}Cl$.

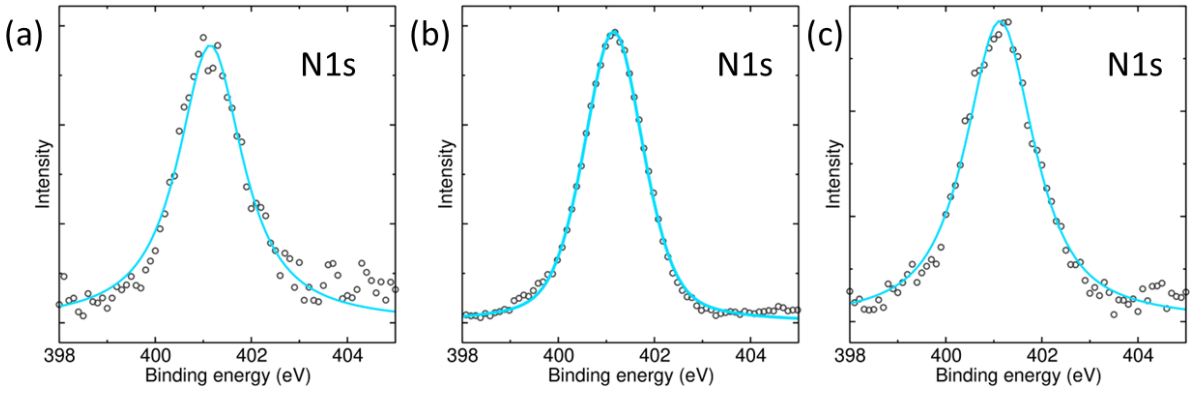

Figure S11: Core level N1s XPS spectra of (a) $(MA)_2AgMoCl_6$, (b) $(1,4\text{-}BDA)_2AgMoCl_8$ and (c) $(MA)_4MoCl_6{\cdot}Cl$, respectively.

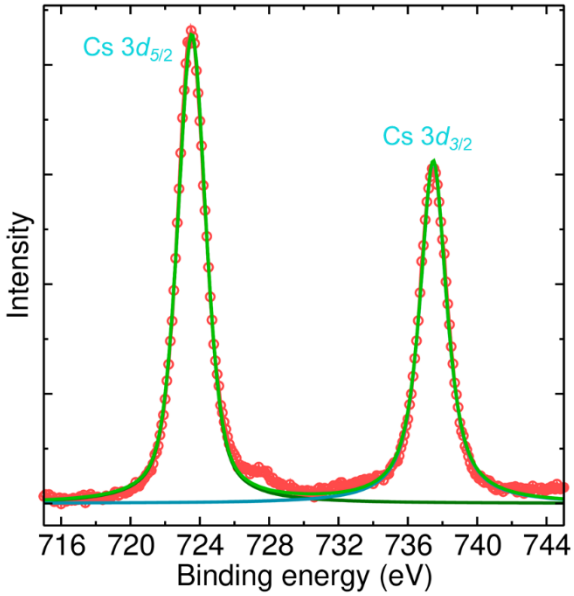

Figure S12: Core level Cs 3d XPS spectrum of $Cs_2NaMoCl_6$.

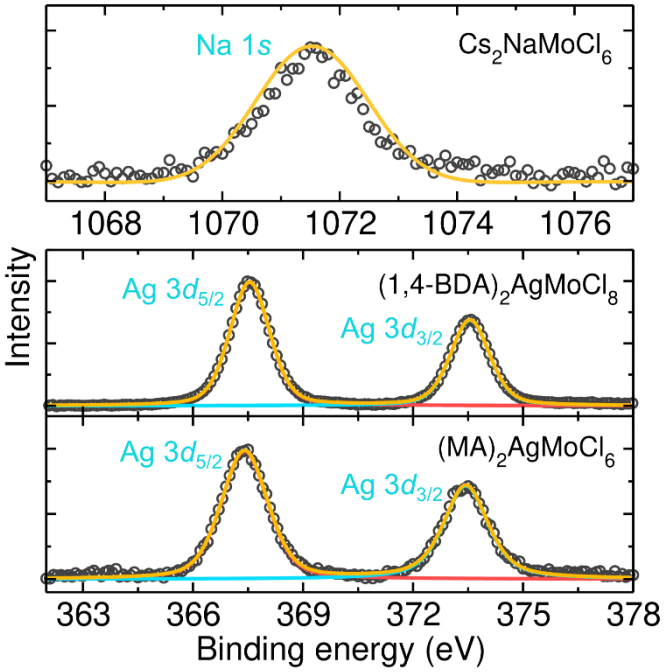

Figure S13: Core level Na 1s XPS spectrum of $Cs_2NaMoCl_6$ and Ag 3d spectra of $(1,4\text{-}BDA)_2AgMoCl_8$ and $(MA)_2AgMoCl_6$.

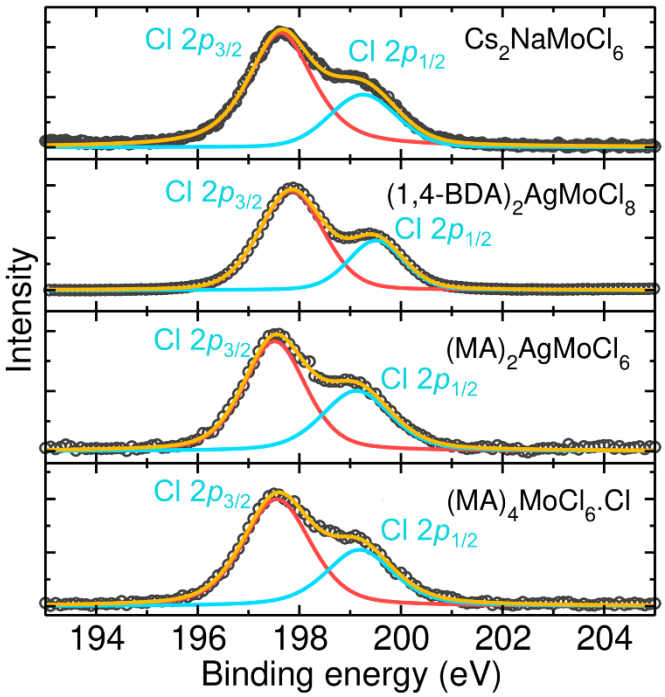

Figure S14: Core level Cl 2p XPS spectra of (a) $Cs_2NaMoCl_6$, (b) $(1,4\text{-BDA})_2AgMoCl_8$, (c) $(MA)_2AgMoCl_6$ and (d) $(MA)_4MoCl_6{\cdot}Cl$.

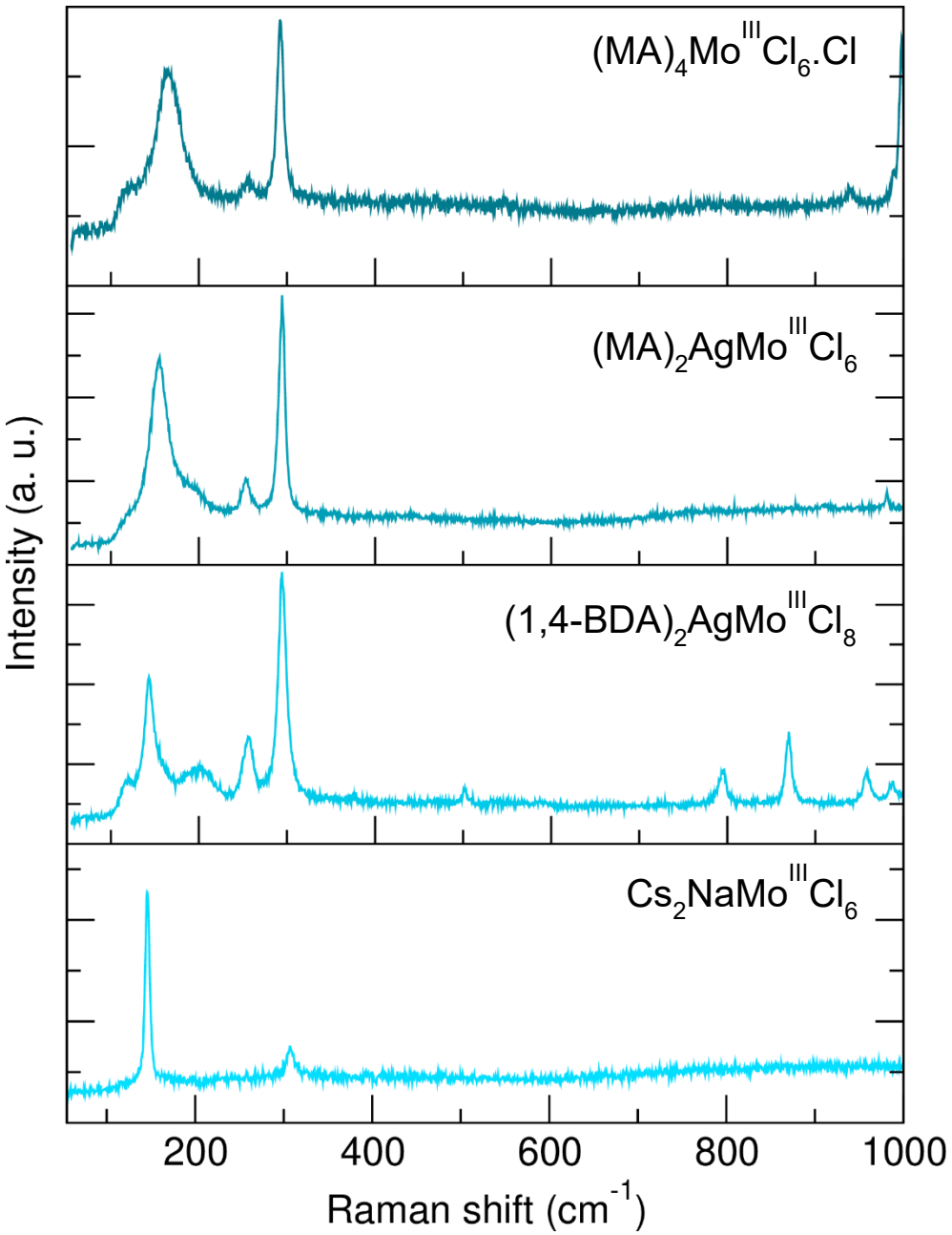

Figure S15: Raman spectra of $Cs_2NaMoCl_6$, $(1,4\text{-BDA})_2AgMoCl_8$, $(MA)_2AgMoCl_6$ and $(MA)_4MoCl_6{\cdot}Cl$.

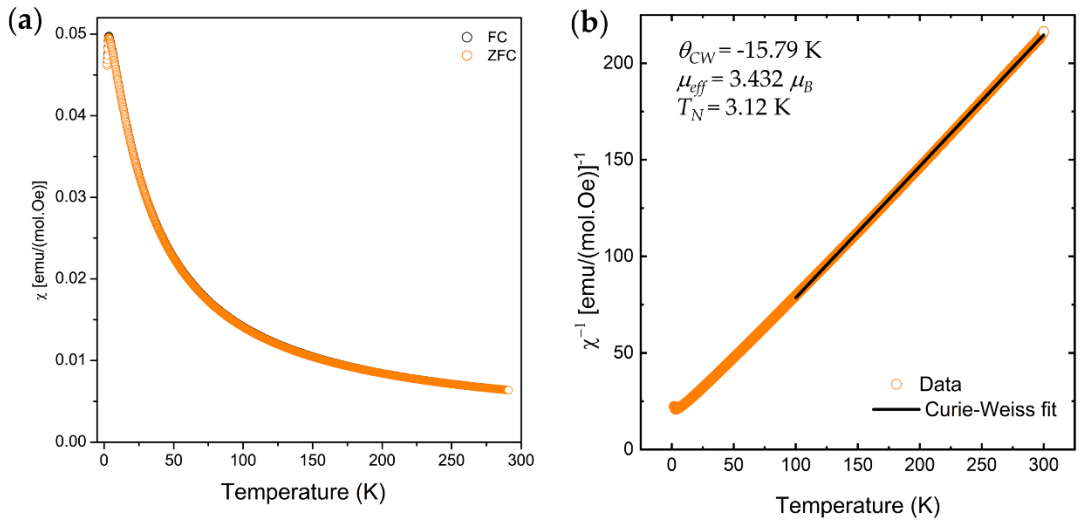

Figure S16: (a) Magnetic susceptibility vs temperature curve for $Cs_2NaMoCl_6$ (**b**) Curve of temperature dependence of the inverse susceptibility of $Cs_2NaMoCl_6$.

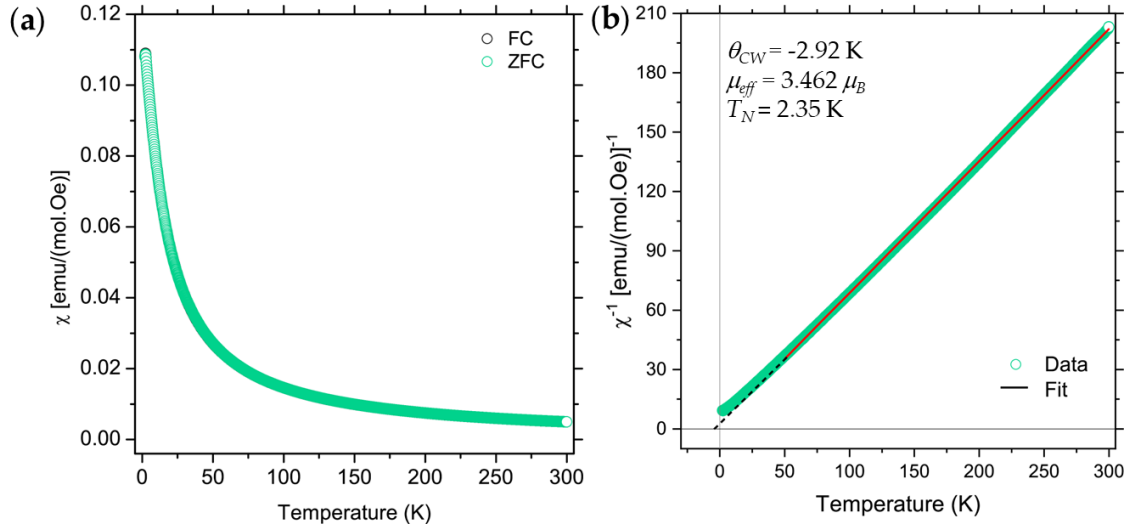

Figure S17: (a) Magnetic susceptibility vs temperature curve for $(MA)_2AgMoCl_6$. (**b**) Curve of temperature dependence of the inverse susceptibility of $(MA)_2AgMoCl_6$.

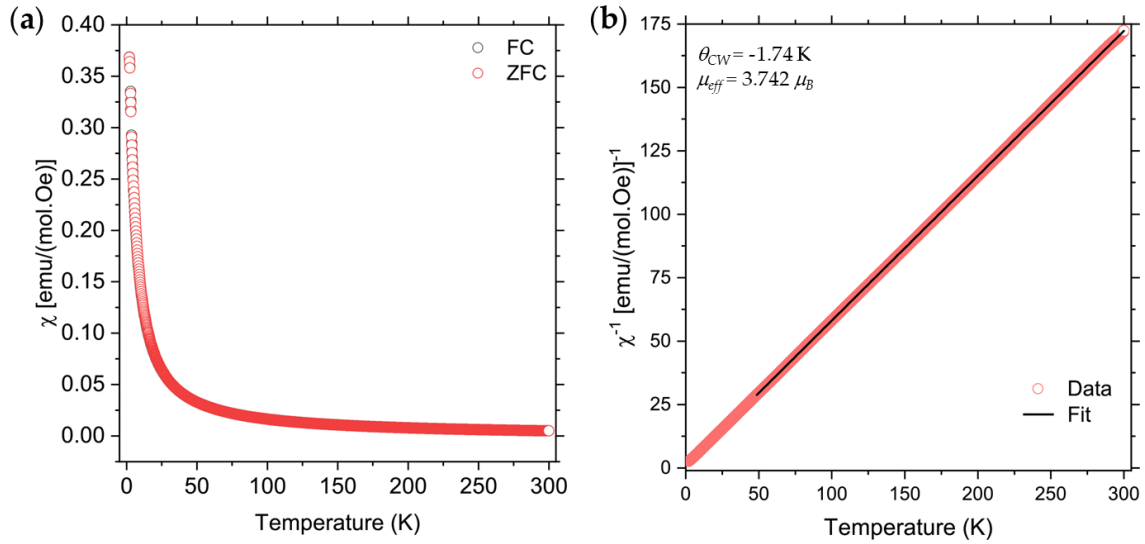

Figure S18: (a) Magnetic susceptibility vs temperature curve for $(1,4\text{-BDA})_2AgMoCl_8$. **(b)** Curve of temperature dependence of the inverse susceptibility of $(1,4\text{-BDA})_2AgMoCl_8$.

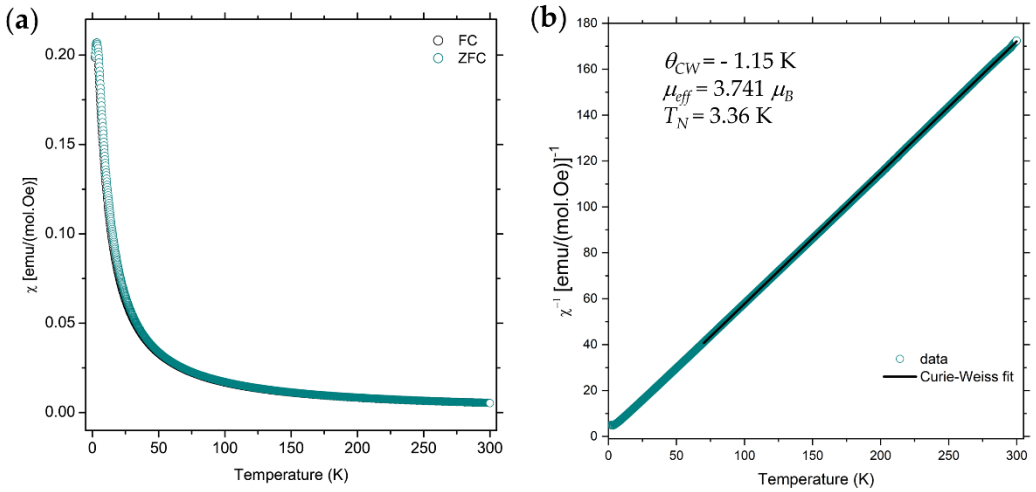

Figure S19: (a) Magnetic susceptibility vs temperature curve for ~~0D~~ $(MA)_4MoCl_6{\cdot}Cl$ **(b)** Curve of temperature dependence of the inverse susceptibility of $(MA)_4MoCl_6{\cdot}Cl$.

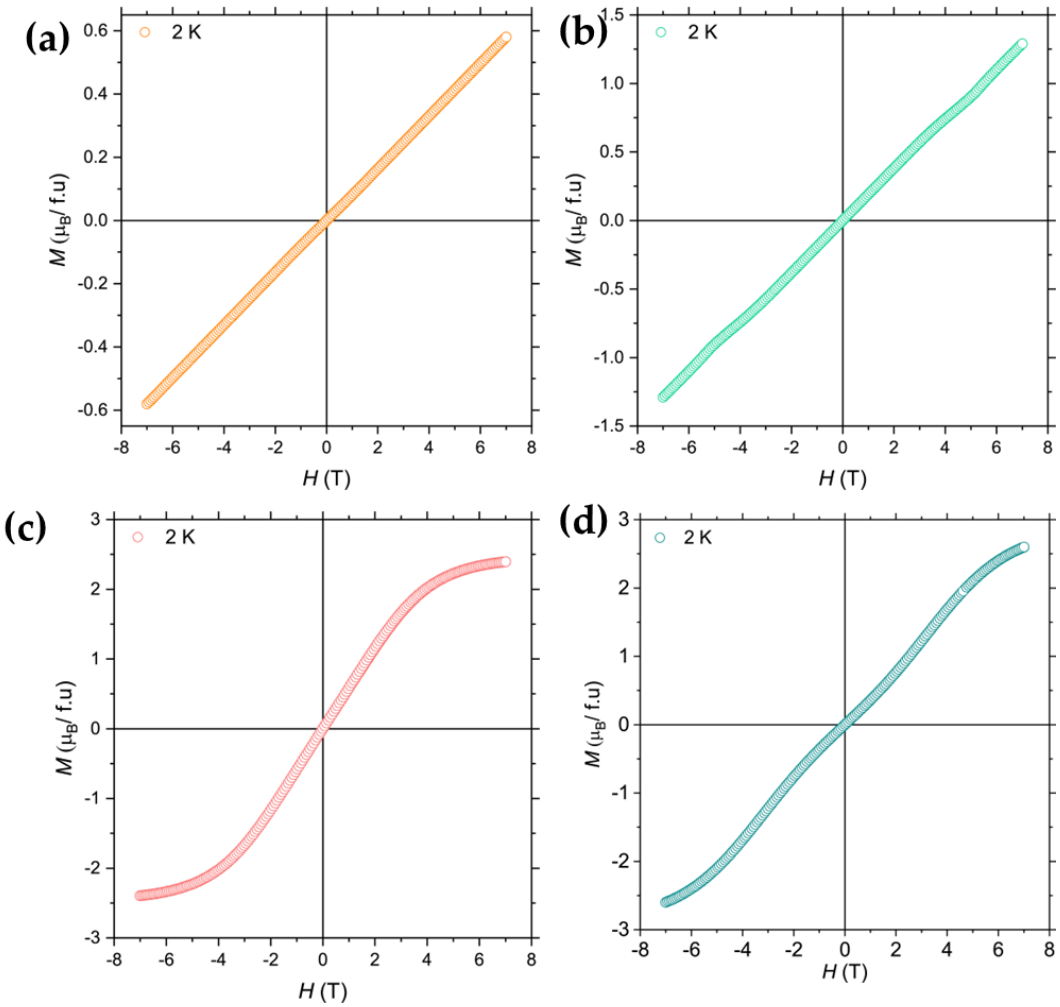

Figure S20: *M* vs *H* curves of (a) $Cs_2NaMoCl_6$, (b) $(MA)_2AgMoCl_6$, (c) $(1,4\text{-}BDA)_2AgMoCl_8$ and (d) $(MA)_4MoCl_6{\cdot}Cl$. (*M* = magnetization; *H* = magnetic field).

Structure of $(MA)_4MoCl_6.Cl$:

$(MA)_4MoCl_6.Cl$ crystallizes in monoclinic phase with *P*2/n *(No. 13)* space group, it contains isolated $[Mo^{III}Cl_6]^{3-}$ octahedra, methylamine cation and chloride anion (Fig S19). Mo-Cl octahedra is slightly distorted with bond length of Mo-Cl in the range of 2.4459(6) Å to 2.4520(8) Å, which is similar to bond length of Mo-Cl in $Cs_2NaMoCl_6$, $(1,4\text{-}BDA)_2AgMoCl_8$ and $(MA)_2AgMoCl_6$**.** PXRD of $(MA)_4MoCl_6.Cl$ has a good match with simulated PXRD pattern, which suggests phase purity of $(MA)_4MoCl_6.Cl$ (Fig. S22).

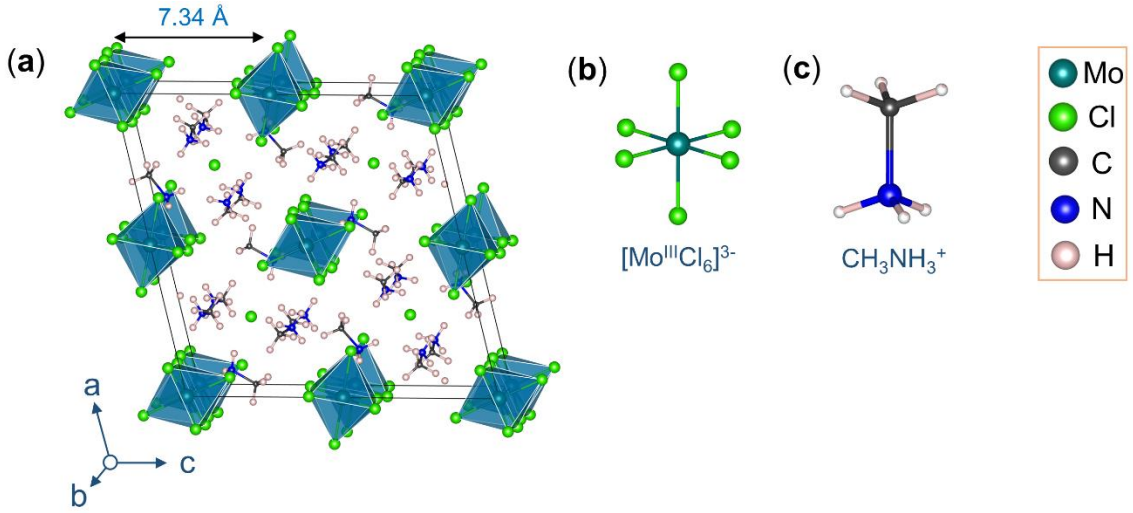

Figure S21: (a) Crystal structure of $(MA)_4MoCl_6{\cdot}Cl$. Ball and stick model of (b) $[MoCl_6]^{3-}$ present in the structure, (c) Methylammonium cation.

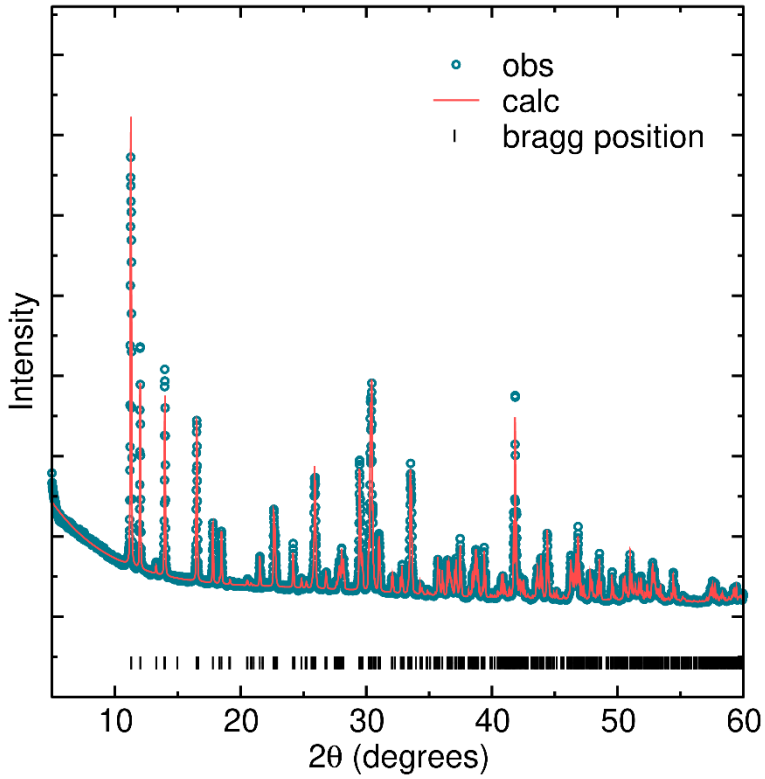

Figure S22: Simulated and experimental PXRD patterns of $(MA)_4MoCl_6 \cdot Cl$.

References:

[1] G. M. Sheldrick, *Acta Crystallogr. Sect. A* **2015**, *71*, 3–8.

[2] K. Momma, F. Izumi, *J. Appl. Crystallogr.* **2011**, *44*, 1272–1276.